applied sciences

MDPI

Article

# Experimental Measurements of the Natural Frequencies and Mode Shapes of Rotating Disk-Blades-Disk Assemblies from the Stationary Frame

**Alexandre Presas *, David Valentin, Carme Valero, Monica Egusquiza and Eduard Egusquiza**

Center for Industrial Diagnostics and Fluid Dynamics (CDIF), Polytechnic University of Catalonia (UPC), Av. Diagonal, 647, ETSEIB, 08028 Barcelona, Spain; david.valentin@upc.edu (D.V.); m.del.carmen.valero@upc.edu (C.V.); monica.egusquiza@upc.edu (M.E.); eduard.egusquiza@upc.edu (E.E.)

* Correspondence: alexandre.presas@upc.edu; Tel.: +34-934-017-132

Received: 3 July 2019; Accepted: 7 September 2019; Published: 14 September 2019


**Abstract:** Determining the natural frequencies and mode shapes of rotating turbomachinery components from both rotating and stationary reference frames is of paramount importance to avoid resonance problems that could affect the normal operation of the machine, or even cause critical damages in these components. Due to their similarity to real engineering cases, this topic has been experimentally analyzed in the past for disk-shaft assemblies and rotor disk-blades assemblies (bladed-disk or blisk). The same topic is less analyzed for disk-blades-disk assemblies, although such configurations are widely used in centrifugal closed impellers of compressors, hydraulic pumps, pump-turbines, and runners of high head Francis turbines. In this paper, experimental measurements, varying the rotating speed of a disk-blade-disk assembly and exciting the first natural frequencies of the rotating frame, have been performed. The rotating structure is excited and measured by means of PZT patches from the rotating frame and with a Laser Doppler Vibrometer (LDV). In order to interpret the experimental results obtained from the stationary frame, a method to decompose the diametrical mode shapes of the structure in simple diametrical components (which define the diametrical mode shapes of a simple disk) has been proposed. It is concluded that the resonant frequencies detected with a stationary sensor correspond to the ones predicted with the decomposition method. Finally, a means to obtain equivalent results with numerical simulation methods is shown.

**Keywords:** natural frequencies; mode-shapes; modal analysis; centrifugal pumps; pump-turbine; closed impellers

## 1. Introduction

Rotating-disk-like structures are a common element in rotating machines (such as circular saws, wafer cutting machines, disk brakes, grinding wheels) and turbomachinery components (blisks, centrifugal fans, gas turbines, hydraulic turbines). These structures are excited by different kinds of dynamic loads and therefore a resonance can occur if the excited frequency coincides with one of the natural frequencies of the structure and the excitation shape matches the mode shape of the structure [1,2]. For this reason, in this kind of rotating structure, it is of paramount importance to predict and determine the natural frequencies and mode shapes of both rotating and stationary frames.

There are many types of rotating structures used in real engineering cases that can be assimilated to a disk-type or disk with blades structure. Some examples of real applications are shown in Figure 1. Figure 1a shows a simple disk, which is basically a circular thin plate. Figure 1b shows a bladed-disk

or blisk, which consists of a central ring with attached blades. Figure 1c is the combination of a simple disk with blades attached to one side. In Figure 1d, a structure that can be considered as an assembly disk-blades-disk is shown. Each type has different mode-shapes and, therefore, their structural response (natural frequencies and mode shapes) has to be studied separately.

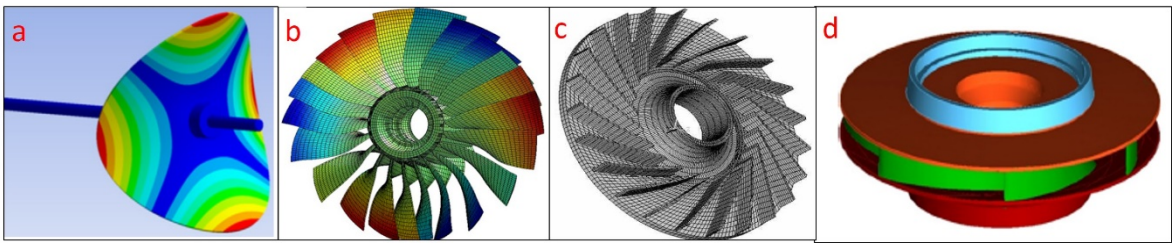


**Figure 1.** Examples of rotating structures involving disks: (**a**) Simple Disk structure [3], (**b**) Bladed disk structure [4], (**c**) Disk-blade assembly [5], and (**d**) Disk-blades-disk assembly [6].

The natural frequencies and mode shapes of simple disks (Figure 1a) have been analyzed in many studies [7–9]. These studies use the governing structural equation of a thin circular plate in order to deduce the natural frequencies and mode shapes of the structure. In [8,9], the characterization of the mode shapes of disk-like structures is defined by the number of nodal diameters (diameters with no deformation) and nodal circles (entire circles with no deformation). This characterization has also been used in many researches on disk-like structures [10–15]. The effect of the rotation for disk-like structures on the natural frequencies and mode shapes can be analyzed from the rotating and stationary frames. When analyzing the structural response from the rotating frame, for simple rotating thin disks, effects such as gyroscopic, centrifugal forces, and shear modify the structural equation at high speeds [16–18]. Therefore, for low rotating speeds, when such effects are not relevant, the structural response of the rotating structure analyzed from the rotating reference frame is almost identical to the structural response of the non-rotating structure. For the same structure rotating at a low rotating speed, when analyzing the structural response from the stationary frame, the following can be observed: Standing mode shapes (observed from the rotating frame) are separated into two travelling modes (stationary frame). The frequency shift between both reference frames depends on the number of nodal diameters of the mode and the rotating speed of the disk [17,19].

Bladed-disks (or blisk), which consist of a rotor disk and blades (Figure 1b), are widely used in the field of stationary gas turbines and in aircraft engines. This kind of structure is said to have cyclic symmetry [20–23], which means that they are composed of identical sectors (each sector contains a part of the disk and the blade). A discussion of the natural frequencies and mode shapes of this kind of structures can be found in [20,21] for "tuned" bladed disks, which means that the condition of cyclic symmetry is accomplished. This mode shape has characteristics of single blade modes (also known as clamped modes) and disk modes. The effects of small differences in the N sectors (mistuning of the bladed-disk) is also discussed in the aforementioned references. The effects of rotation on the natural frequencies are discussed in [23] for the rotating and stationary frames.

For disk-blades configurations (Figure 1c), there is less literature on the structural response (natural frequencies and mode shapes) and associated dynamic problems. These type of structures are typically used as the centrifugal impellers of some small compressors and also in small centrifugal water pumps (semi-open impeller). In this case, the mode shapes of the disk-part become more important (since blades are clamped at its longer dimension) and they appear usually as the first and more excitable mode shapes [5,24,25]. Nevertheless, blade modes are also considered in some of these studies [5,25].

Finally, disk-blades-disk assemblies (Figure 1d), which are the type of structures analyzed in this paper, are present in closed centrifugal impellers (with working fluid air and water) and high head Francis runners, as seen in Figure 2. The several first mode shapes of these structures are dominated by the disk-part (blades are doubly clamped), which indicates mode shapes with deformation in the traverse direction to the disk plane [6,26–33]. In the aforementioned references, the diametrical

modes (modes with nodal diameters) are particularly considered, because they are the lower modes in frequency and the most prone to be excited. For this reason, the same characterization using nodal diameters as in simple disks is used. Nevertheless, defining the mode shapes of disk-blades-disk assemblies with a single number of nodal diameters is inadequate, since the mode shapes are not perfectly sinusoidal (as the theoretical modes in a simple disk), and this may lead to simplified predictions of the resonant peaks detected from the stationary frame.

In this kind of structure, the rotational speed is relatively low [30,34]. Therefore, it is expected that when analyzing the natural frequencies and mode shape from the rotating frame (considering the structure rotating in vacuum or a low-density fluid), effects such as gyroscopic and centrifugal forces modify the structural equation slightly and the natural frequencies do not change. Studying the problem from a stationary frame is advantageous, since, experimentally, it is much more feasible to place sensors in that reference frame. As mentioned before, for simple disks structures, this problem has been deeply analyzed. Particularly, the natural frequencies corresponding to diametrical mode shapes are separated from the natural frequency measured on the rotating frame with a frequency shift depending on the number of nodal diameters and the rotating speed of the disk [17,19]. Nevertheless, no experimental or numerical studies have been found where the same problem is studied for the structural behavior of disk-blades-disk assemblies. It is also to be mentioned that analysis of the excitations from the stationary point of view, occurring in a type of disk-blade-disk assemblies (Francis turbines and pump turbines), has been discussed in some studies, such as by Zobeiri [35] or Nicolet et al. [36].

Computationally, it is easier to predict natural frequencies and mode shapes with commercial numerical codes [19,30–32], but it may be difficult to predict natural frequencies from the stationary frame when the structure is rotating. For such cases, typical commercial software (ANSYS® [37], MSC NASTRAN® [38]) impose the restriction that analysis from the stationary frame can be only done for axisymmetric structures. Particularly, both codes share the same restrictions, according to the respective reference handbook [37,38].

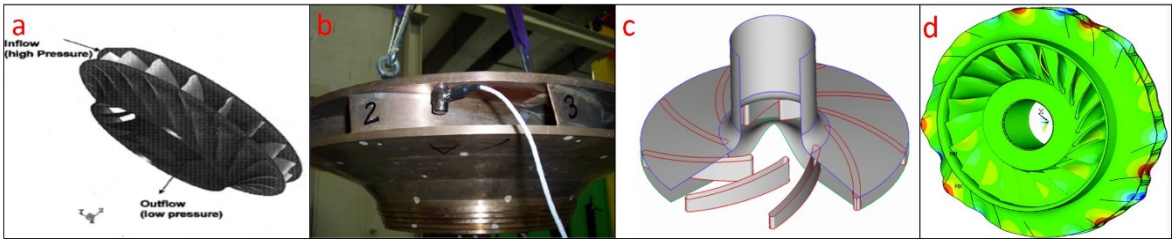


**Figure 2.** Real engineering cases where disk-blades-disk assemblies are used. (**a**) Low specific speed Francis Turbine runner [39], (**b**) Pump-turbine impeller [40], (**c**) Centrifugal pump impeller [41], (**d**) Centrifugal compressor impeller [42].

As can be seen in Figure 2, disk-blades-disk assemblies are generally non-axisymmetric, due to the curvature of the blades and, therefore, according to Table 1, the natural frequencies from the stationary frame cannot be directly obtained with such computational codes. Nevertheless, to overcome such a problem for the first several mode shapes, which are strongly dominated by peripheral disk modes (maximum deformation on the periphery and no nodal circles [14]), an option could be to discompose the mode shapes as a superposition of diametrical modes found in simple disks.

In this paper, an analytical method to precisely characterize the diametrical mode shapes of disk-blades-disk assemblies is proposed. Furthermore, it is shown how to use this characterization to predict the natural frequencies observed from the stationary frame. Diametrical mode shapes (modes with no nodal circles), which are the several first mode shapes for this kind of structure, are analyzed from the rotating frame. A method to decompose the diametrical mode shapes in simple diametrical components (such as in a disk) is developed and used. Based on this decomposition, the natural frequencies relative to the stationary frame can be analytically predicted. The problem is also studied

experimentally with a rotating disk-blades-structure in a test rig. The test rig allows to excite the structure from the rotating frame and measure the response from both rotating and stationary frames, simultaneously. The rotating structure is also analyzed by means of experimental and numerical modal analysis. The proposed method in this paper is used to decompose the several first diametrical modes of the rotating structure and to predict the natural frequencies detected with a stationary sensor.

**Table 1.** Restrictions of the numerical analysis of typical commercial codes (ANSYS® [37], MSC NASTRAN® [38]).

| Stationary Frame | Rotating Frame |
|---|---|
| Rotating structure has to be axisymmetric around the rotating axis | Rotating structure can be not axisymmetric around the rotating axis |
| Rotating structure can be connected to stationary structures | Only rotating structure can be considered in the analysis |
| More than one rotating structure | Only a single rotating structure |
| Campbell diagrams for computing rotor critical speeds are possible | Campbell diagrams are not applicable |
| | Cyclic-symmetric analysis can be used |

## 2. Diametrical Mode Shapes of Rotating Disk-Blades-Disk Like Structures from the Rotating Frame

Firstly, the rotating structure is analyzed from the rotating reference frame. If the structure rotates at relative low rotating speeds and is surrounded by low density fluid in comparison with the material of the rotating structure (usually steel), the influence of the surrounding flow, inertia, shear, and gyroscopic effects can be neglected [43]. In this case, it can be assumed that the mode shape analyzed from the rotating frame is the same as in the standing case. The simple disk case is introduced to understand the more complex case of the disk-blades-disk assembly.

### 2.1. Simple Disk Case

Considering that all the points are moving in phase or in counterphase to each other (real mode shape), the deformation of a disk can be written as [8,44]:

$$w(r,\theta,t) = \sum_{n=0}^{\infty}\sum_{m=0}^{\infty} W_{nm}(r)\cos(\mathrm{n}\theta)\cos(\omega_{nm}t) \quad (1)$$

where $w$ is the transverse deformation (perpendicular to the plane of the disk), $r$ the radial position, $\theta$ the angular position and $t$ time. $W_{nm}$ is a function that involves the use of Bessel functions [8,9]. $n$ is the number of nodal diameters and m the number of nodal circles. Figure 3 shows the generic transverse motion (in $z$ direction) of a generic disk-like structure in cylindrical coordinates.

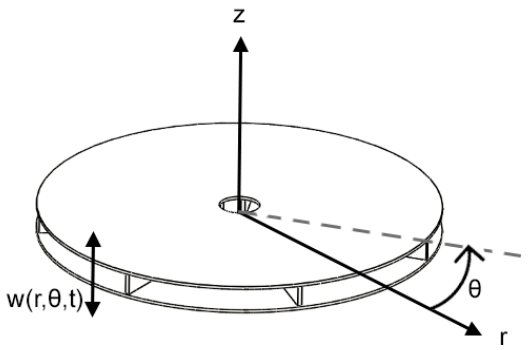


**Figure 3.** Coordinates for a generic disk-like structure.

For a thin disk clamped at its center (clamped by the rotating shaft) with high outer to inner radius ratio, the first mode shapes are usually diametrical modes (modes with no nodal circles, i.e., $m$ = 0) [8,9,13]. These modes are also usually the most prone to be excited in centrifugal impellers [30,31,40], and for this reason will be the modes considered in this paper. Therefore and for simplicity, $\omega_n$ will be used instead of $\omega_{nm}$. For these kind of modes, the deformation at the periphery is larger than that in the more inner radii. Consequently, the peripheral deformation will be used to characterize the diametrical mode shapes.

From Equation (1), considering that $t$ = 0, all the points pass through their maxima to minimum ($\cos(\omega_{nm}t) = 1$ for $t$ = 0) and considering that there is a local maximum for $\theta = 0$, the deformation on the periphery at this time can be expressed as:

$$w_{p,n}(r = r_{max}, \theta, t = 0) = A_n \cos(\mathrm{n}\theta) \tag{2}$$

where $w_{p,n}$ is the deformation on the periphery (p) for the n diametrical mode and $A_n$ the amplitude of vibration of the corresponding mode, which depends on the angular position $\theta$. From Equation (2), it can be seen that each mode has a single $\cos(n\theta)$ component, which defines the diametrical mode n.

For other $t$, where the points are not passing through its maximum/minimum, $w_{p,n}$ will be lower than for $t$ = 0. Nevertheless, since all the points are moving in phase or in counterphase to each other (same term $\cos(\omega_{nm}t)$ in Equation (1)), the deformation shape will be proportional to the deformation at $t$ = 0 and, therefore, the deformation shape on the periphery at any time is representative of the mode shape (except for $t = \frac{\pi}{2\omega_{nm}}, \frac{3\pi}{2\omega_{nm}}$ where all the points pass through 0). An example of the peripheral deformation of this kind of structure can be seen in Figure 4a.

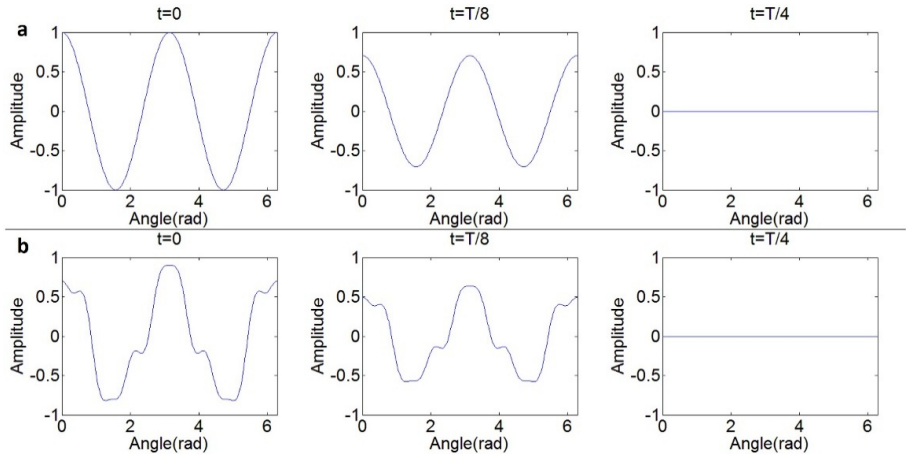


**Figure 4.** $w_{p,n}$ for different times. (**a**) Mode $n$ = 2 of a simple disk structure (one diametrical component). (**b**) Mode with more than one diametrical component.

### *2.2. Disk-Blades-Disk Structures*

Since there are many factors that can determine the mode shapes of a disk-blades-disk structure (number and geometry of the blades, junctions blade-disk ... ), there is not a standard analytical form to describe the mode shapes of these structures.

In this paper, the type of structure disk-blades-disk, which is used for closed impellers in centrifugal compressors, pump-turbines, centrifugal pumps and low specific speed Francis runners [30,34,39,42], is analyzed in detail.

Considering again the diametrical modes and assuming that these are real modes (points are moving in phase or in counterphase to each other), the deformation at the periphery, when all the points pass through their maxima/minima (supposing this for $t$ = 0), can be written in a general form:

$$w_{p,i}(r = r_{max}, \theta, t = 0) = A_i(\theta) \text{ for } 0 \leq \theta \leq 2\pi \tag{3}$$

In this case, the deformation at the periphery of the mode $i$ is not pure sinusoidal as for the simple disk case, due to the blades. Nevertheless, for a diametrical mode, again the deformation at the periphery is larger than the inner radii. In this case, the deformation at the periphery is defined by an arbitrary function $A_i$, which depends on the angular position $\theta$. Once more, for any other time $t$, the deformation will be lower than that expressed in Equation (3), but it will be proportional.

Note that $i$ is used instead of $n$, since it is assumed that, generally, the mode cannot be defined by a single number of nodal diameter $n$ (otherwise $cos(n\theta)$ would be used, as in a simple disk). Nevertheless, no matter how complex the peripheral deformation is, there is a periodicity on the mode shape deformation if the entire periphery is considered ($A_i(\theta = 0) = A_i(\theta = 2\pi)$), which means that the deformation in Equation (3) can be rewritten using Fourier series in their compact form [45]:

$$w_{p,i}(r = r_{max}, \theta, t = 0) = A_i(\theta) = \sum_{n=0}^{\infty} A_{n,i} \cdot \cos(n\theta + \varphi_n) \quad (4)$$

As seen in Equation (4), the deformation is expressed as the sum of single components that are characterized by the number of nodal diameters n, with amplitude $A_{n,i}$ and phase shift between components of $\varphi_n$. Each single term has the same deformation pattern as a single disk diametrical mode shape (Equation (2)). An example of this kind of deformation with more than one diametrical component can be seen in Figure 4b.

In real engineering applications, these types of structures are clamped to a shaft. The influence of clamping a disk-like structure, on the first diametrical modes with $n \geq 2$, which are the first diametrical modes appearing disk-blade-disk structures, is almost negligible, especially for $n > 2$ [8]. Many references show that the first modes of a real disk-blade-disk configuration [6,31–33,40] are dominated by disk-modes and therefore the effect of the clamping is also to slightly increase the first diametrical mode shapes without modifying the main characteristics of the mode shape, i.e., the aforementioned characteristics of the diametrical mode shapes are still the same.

Other effects, such as mistuning, which plays an important role in blade-disk configurations (blisk) for blade dominated modes, are less important for mode shapes that exhibit a shape similar to simple diametrical disk mode shapes [20]. The main effect of a possible mistuning is to separate the doublets in frequency [20], although in many real cases, this separation is less than 1% with respect to the natural frequency value [6]. However, in case the two existing doublets are clearly separated, they will keep the main characteristic of a diametrical mode shape and therefore can be separately considered and discomposed with the following method.

## 3. Decomposition of the Diametrical Mode Shapes for Disk-Blade-Disk Configuration

A method to characterize the diametrical mode shapes of disk-blades-disk structures is proposed in this section. This method helps to have a better knowledge of which diametrical components are participating in a diametrical mode shape of the structure.

As mentioned before, based on the ideas of the Fourier transform for periodical functions, the deformation at the periphery can be discomposed as a sum of single diametrical components, which characterize the diametrical modes of simple disk structures. Assuming that the diametrical mode shape is real (all points moving in phase or counterphase to each other), it is enough to discompose the periphery at the time when the deformation of all the points is at its maximum ($t = 0$ for Equation (3)).

Mode shapes obtained experimentally or by means of numerical simulation are generally measured in a number of discrete points. Therefore, the discrete version of the Fourier transform (i.e., the FFT algorithm [45]) is used. To exemplify the method in order to discompose a diametrical mode shape, it will be applied to discompose a diametrical mode shape of a simple disk obtained with numerical simulation (Figure 5):

- It is assumed that the response is measured in $N'$ equidistant points.

- In order to get a good resolution in the diametrical components information, this deformation is virtually elongated λ times (10 times in this example) in space. The first and the last point of the final sequence correspond to the displacement at angle 0° (Figure 5b).

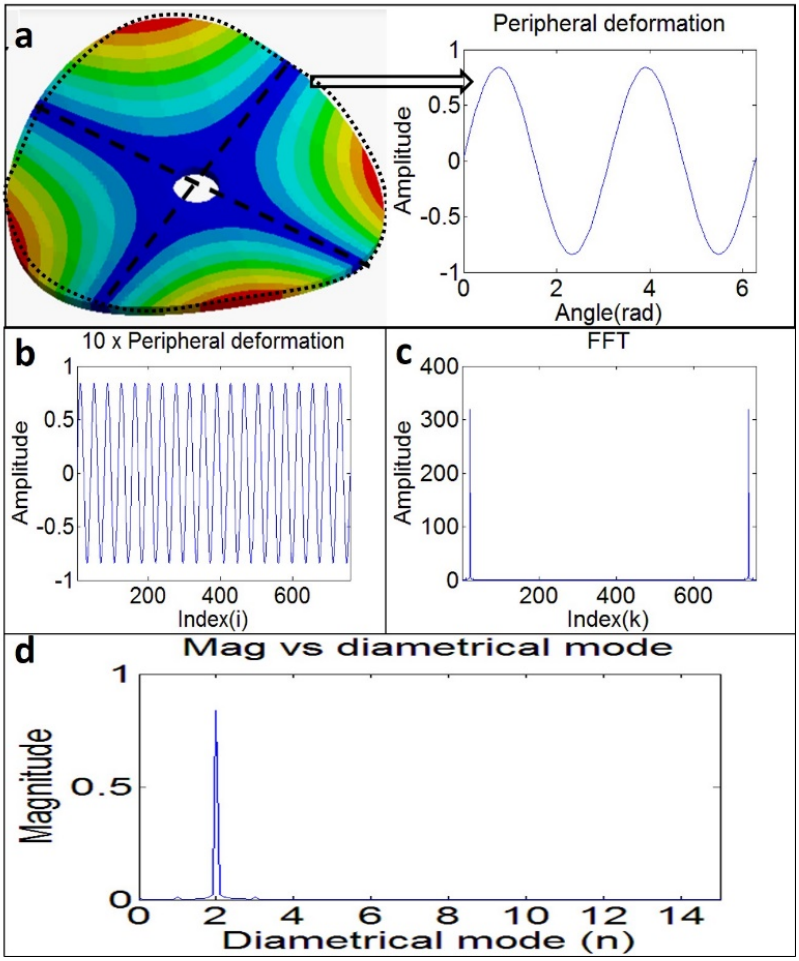


**Figure 5.** Procedure of mode shape decomposition: (**a**) Periphery of the disk, (**b**) Periphery elongated 10 times, (**c**) Magnitude after applying FFT algorithm, (**d**) Magnitude vs. Diametrical component.

- The FFT is applied to the resulting peripheral deformation. The transform is according to the following equation:

$$X_k = \sum_{i=1}^{N} X_i e^{-j2\pi k \frac{i-1}{N}} \; for\, k = 1, \ldots, N \tag{5}$$

- In this equation $X_i$ is the sequence of points of the elongated periphery that has $N$ points. $X_k$ is the sequence of complex values after the transformation (Figure 5c).
- The first $N/2$ values of the sequence $X'_k$ are plotted in Magnitude against the diametrical components. To do this, the following transformation with the index $k$ has to be done.

$$n = \frac{k-1}{\lambda} \tag{6}$$

$n$ represents the diametrical components. In this case, λ = 10 is considered, because the peripheral deformation is elongated 10 times. The magnitude is represented in terms of 0-peak value and, therefore, to obtain $X'_k$ from the $X_k$-values:

$$X_k' = X_k \cdot 2/N \tag{7}$$

It is useful to notice the following consequences:

- The resolution in the diametrical components is 1/λ, where λ is the number of times that the peripheral deformation is virtually elongated. To accurately see the diametrical components, λ should be higher or equal to 2 (λ ≥ 2).
- The maximum diametrical component that can be detected on the mode shape depends on the number of measured points on the periphery (equidistant points). $n_{max} = N'/2$ where $N'$ is the number of measured points on the periphery.

For the example case, it is clearly seen (Figure 5d) that the unique diametrical component in the analyzed mode shape is the component $n = 2$. This number indicates the number of nodal diameters in this diametrical mode, which is also appreciated in Figure 5a.

*Application of the Decomposition in a Real Prototype Disk-Blades-Disk Structure*

This section shows the application of the method in a real prototype disk-blades-disk structure (Figure 6a). The structure is a pump-turbine impeller with seven curved blades. The diameter is approximately 3 m. This structure has been analyzed in previous researches [6,30]. Only a diametrical mode of the structure is shown here as an example. The peripheral deformation of this mode is obtained by means of numerical simulation and through experimental modal analysis (Figure 6b). The amplitude of this deformation is normalized to 1 in both cases. The decomposition of the mode shape applying the methodology explained before is shown in Figure 6c.

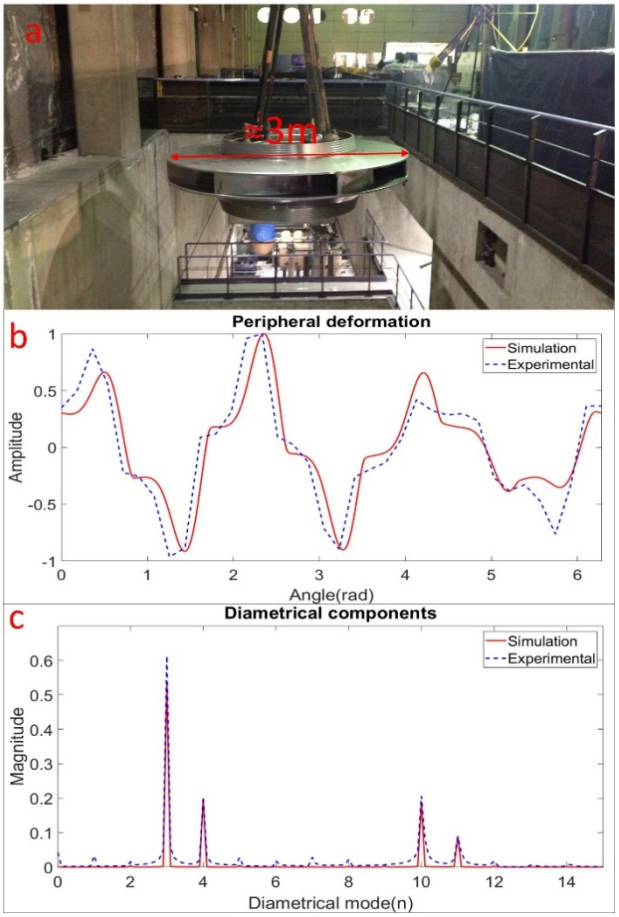


**Figure 6.** Diametrical mode of a real impeller (non-rotating structure): (**a**) Impeller analyzed, (**b**) Peripheral deformation of the diametrical mode with main component $n = 3$, (**c**) Amplitude of the components obtained with mode shape decomposition.

It can be seen that, apart from the main component $n$ = 3 (therefore, in the aforementioned references the mode is described as 3ND), other components such as $n$ = 4, 10, 11 are also found in the decomposition. Generally, these structures exhibits multiple components instead of a single diametrical component that simple disk-like structures have (Figure 5) [43]. Therefore, it is shown that the description of these mode shapes with a unique diametrical mode component [6,26–33] is incomplete. The next section shows the consequences of the natural frequencies detected with a stationary sensor, when the disk-blade-disk structure is in rotation.

## 4. Diametrical Mode Shapes of a Rotating Disk-Blades-Disk Structure Observed from a Stationary Point of View and Its Relation to Mode Shape Decomposition

This section shows the analytical relation between the components obtained with mode shape decomposition and the natural frequencies observed with a sensor on the stationary frame. Figure 7 helps us to understand the underlying problem.

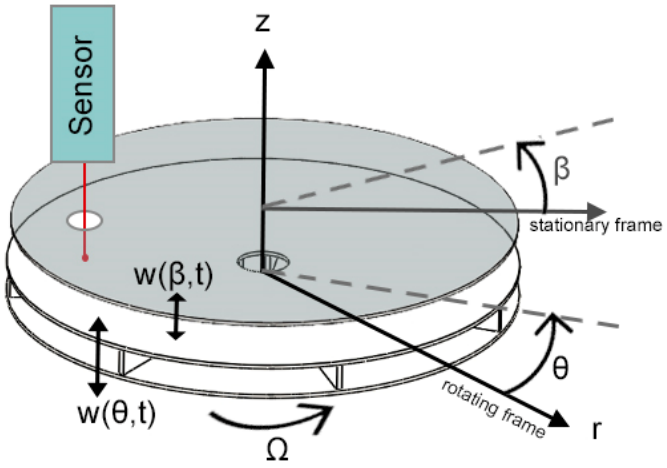


**Figure 7.** Rotating and stationary frame.

A sensor placed on the stationary reference frame (for example, a Laser Doppler Vibrometer) measures the transverse vibration of the rotating structure. As mentioned before (Section 2), for a structure rotating at low rotating speeds (neglecting inertia, shear and gyroscopic effects), it can be assumed that the mode shape in the standing case is the same as in the rotating case (considering the mode shape from the rotating frame), and also that the resonant frequency is approximately the same as in the standing case [43].

If the deformation of the $i$-diametrical mode of the bladed-disk is analyzed from the rotating frame [19,43]:

$$w_{p,i-rot}(\theta,t) = A_{i-rot}(\theta)\cdot\cos(\omega_{i-rot}t) \tag{8}$$

In this section, subscripts "-rot" and "-stat" will be used to emphasize the difference between both reference systems. Using Equation (4), Equation (8) can be rewritten as:

$$w_{p,i-rot}(\theta,t) = \sum_{n=0}^{\infty} A_{n,i-rot}\cdot\cos(n\theta+\varphi_n)\cdot\cos(\omega_{i-rot}t) \tag{9}$$

If the resonance is analyzed from an observer on the stationary frame, the angular coordinate θ (on the rotating frame) is changed for angular coordinate $\beta$ (on the stationary frame) [19] with the following change of reference frame (Figure 7):

$$\beta = \theta + \Omega\cdot t \tag{10}$$

This transformation is substituted in Equation (9) obtaining the peripheral deformation observed from the stationary frame:

$$w_{p,i-stat}(\beta,t) = \sum_{n=0}^{\infty} A_{n,i-rot} \cdot \cos(n(\beta - \Omega \cdot t) + \varphi_n) \cdot \cos(\omega_{i-rot} t) \tag{11}$$

For simplicity, it will be assumed that the sensor on the stationary frame is located at $\beta = 0$. This assumption does not affect the frequency content of the function above. In this case, Equation (11) can be rewritten as:

$$\begin{aligned} w_{p,i-stat}(\beta,t) = & \sum_{n=0}^{\infty} \frac{A_{n,i-rot}}{2} \cdot \cos((\omega_{i-rot} + n\Omega)t - \varphi_n) \\ & + \sum_{n=0}^{\infty} \frac{A_{n,i-rot}}{2} \cdot \cos((\omega_{i-rot} - n\Omega)t + \varphi_n) \end{aligned} \tag{12}$$

From Equation (12) it can be extracted that the frequencies that will detect a sensor on the stationary frame are:

$$\omega_{i-stat} = \sum_{n=0}^{\infty} \omega_{i-rot} \pm n\Omega \tag{13}$$

And each of these frequencies will appear with an amplitude:

$$A_{n,i-stat} = \frac{A_{n,i-rot}}{2} \; for \; n \neq 0 \; and \; A_{n,i-stat} = A_{n,i-rot} \; for \; n = 0 \tag{14}$$

It should be noted that Equation (13) does not impose a restriction on $n$. Nevertheless, only the components ($n$), that appear with a relevant amplitude ($A_{n,i-rot}$), will really produce a peak-frequency in the stationary sensor. In the particular case of a simple disk, with only one component for each diametrical mode shape, only two peaks will be observed with a sensor on the stationary frame [17,19]. However, for the analyzed structures in this paper, two frequencies for each component of the mode-shape are expected to be detected from the stationary frame, according to Equation (13).

The mode shape decomposition proposed in the previous section gives the relative importance that each component $n$ has on the analyzed diametrical mode shape. This means that the different $A_{n,i-rot}$ participating in the mode shape can be obtained with the proposed decomposition. Hence, the relation to the components obtained with the mode shape decomposition and the frequencies seen from a sensor on the stationary frame is proven in this section. Similar equations to describe the periphery of blade-disk configurations as a superposition of diametrical modes have also been used in the past [46].

## 5. Experimental Test

To experimentally validate the main conclusions of the methodology proposed in Section 3 for the decomposition of the mode shapes of the rotating disk-blades-disk structure, and its relation with the frequencies seen from the stationary frame (Section 4), a rotating disk-blades-disk test rig has been developed. It consists of a disk-blades-disk assembly, which rotates inside a rigid casing. The structure is excited with a piezoelectric patch (PZT) from the rotating frame and the response is measured simultaneously from the rotating frame with another PZT, and from the stationary frame with a Laser Doppler Vibrometer (LDV).

### *5.1. Test Setup*

The test rig setup consists of a test rig with a disk-blades-disk structure that can rotate in the range of some kind of real turbomachinery (0–15 Hz), which use this kind of assembly. As mentioned before, this kind of assembly is used basically in closed impellers of pump turbines, pumps, centrifugal compressors, and low specific speed Francis runners [30,34,39,42].

The structure used for the test rig is a double disk (200 mm radius and 3 mm thickness) with seven straight blades (4 mm thickness) welded on it (Figure 8). Since the bladed-disk structure is thin, (low mass per surface) and to not affect the dynamic response of the structure with the instrumentation (load mass of sensors and actuators [47]), an accurate selection of the sensors and actuators has been made. For this purpose, two piezoelectric patches (one in the upper disk and the other in the lower disk) were glued to the disk with an epoxy component (LOCTITE 454). The PZTs (P876 A12) have a surface of 61 × 35 mm and its weight is 0.1 g.

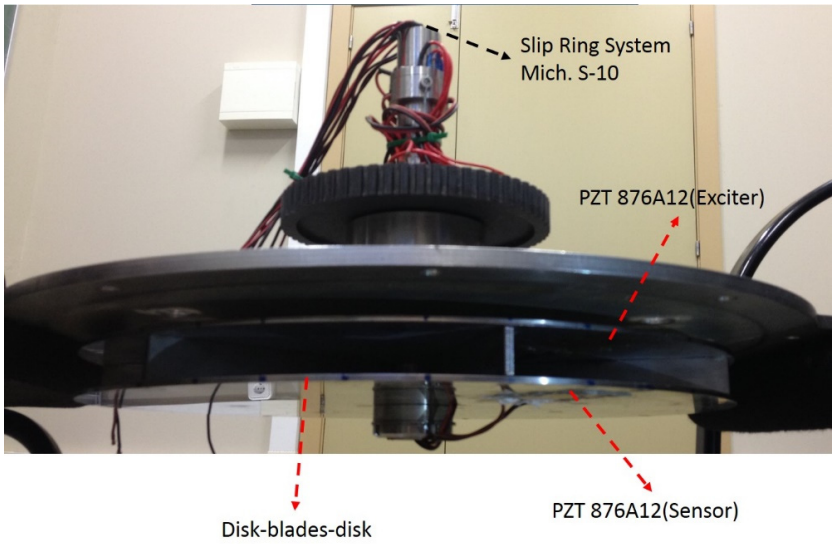


**Figure 8.** Experimental setup.

The PZT on the upper face is used to excite the disk and the PZT on the lower face is used to measure the dynamic response (Figure 8). Simultaneously, the response of the rotating structure is measured with a Laser Doppler Vibrometer (PDV-100) (for simplicity, it is not shown in Figure 8, but sketched in Figure 7). The signals are transmitted to the stationary frame through a slip ring Michigan S-10, located at the tip of the shaft (Figure 8).

The motor is a Mavilor MLV-072, which is a variable speed motor. The rotating speed is controlled with a resolver (Mavilor Resolver 2T8) and can be adjusted with precision of 1/300 Hz. The vibrations of the motor are isolated from the rest of the test rig trough rubber mounting isolators installed between the motor support and the test rig. More details on this test rig (but used for a simple disk) and the instrumentation can be found in [19].

### *5.2. Mode Shape Decomposition of the Diametrical Modes for the Standing Disk-Blades-Disk Structure*

In order to use mode shape decomposition for the diametrical modes of disk-blades-disk assemblies, presented in Section 3, the several first modes of the structure are determined experimentally for the non-rotating case. For this purpose, the following procedure is done: The structure is excited with the upper PZT using a chirp signal of 4 s. The response is measured with the other PZT (used as sensor) and with the Laser Doppler Vibrometer (LDV), which is directly pointing to some point of the periphery on the upper surface of the disk-blades-disk. For one position of the Laser, the excitation is applied five times to check the repeatability of the experiments and the coherence between signals.

Once the experiment is performed for one position of the Laser, the structure is turned to an angle of $2\pi/35$ rad. The aforementioned procedure is repeated for this position, and so on. Therefore, after one complete turn of the structure, the deformation on the periphery is obtained in 35 equidistant points (Figure 9).

Figure 10 shows the excitation signal, the response measured with the PZT, and the response measured with the LDV when the LDV is directed to point 1 (Figure 9).

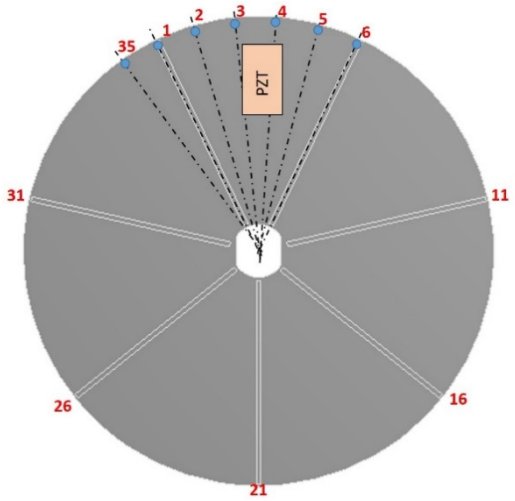


**Figure 9.** Modal analysis of the bladed disk. Positions measured with the LDV.

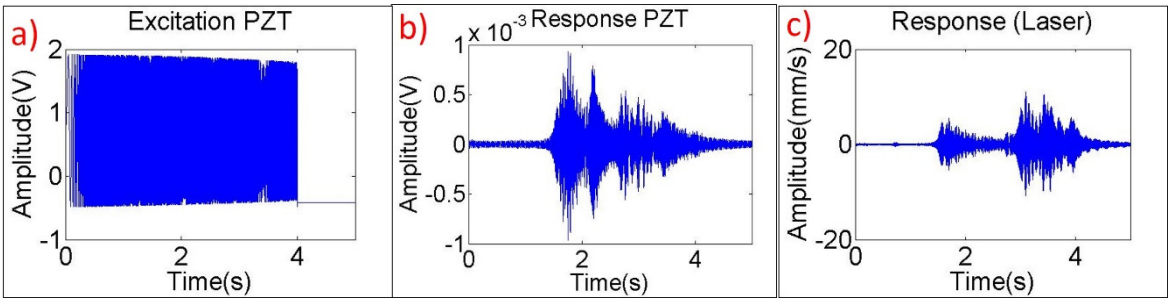


**Figure 10.** Time signals. (**a**) Signal PZT exciter, (**b**) Signal PZT sensor, (**c**) Signal Laser.

After acquiring the time signals for the 35 points, the Frequency Response Functions (FRF) were obtained. In the calculated FRFs, the signal of the LDV is used as a response and the signal of the PZT (exciter) is used as a reference signal. The FRFs using the PZT (sensor) as a response and PZT (exciter) as a reference are also calculated to check the repeatability of the experiments. Figure 11 shows the FRF of the LDV and the FRF of the PZT for two different positions of the LDV. The modes shown in this figure are diametrical modes, which will be analyzed in the standing case and in the rotating case (following section). As can be seen, when changing the measured point, the response of the LDV obviously changes (Figure 11a), while the response of the PZT (Figure 11b) does not (since the only change between both tests is the focusing position of the LDV). Therefore, in Figure 11b, both lines appear almost overlaid. This validates the repeatability of the experiments and the use of both PZTs for the rotating case.

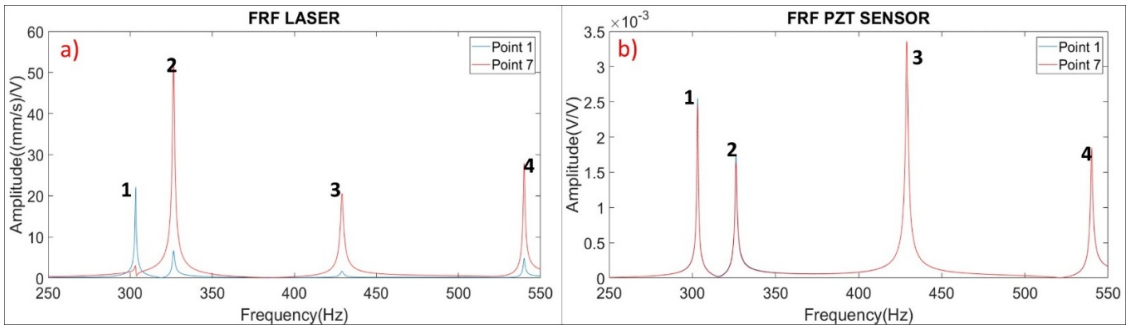


**Figure 11.** Analyzed diametrical modes. Experimental response of the structure measuring different positions of the bladed-disk with the LDV (**a**) and the PZT (**b**). Standing structure (not rotating).

With the FRFs of the 35 points on the periphery in the experimental case, the Operating Deflection Shape (ODS) in the axial direction is obtained. As an example, the deformation of the second mode (326 Hz, Figure 11) is shown in Figure 12a.

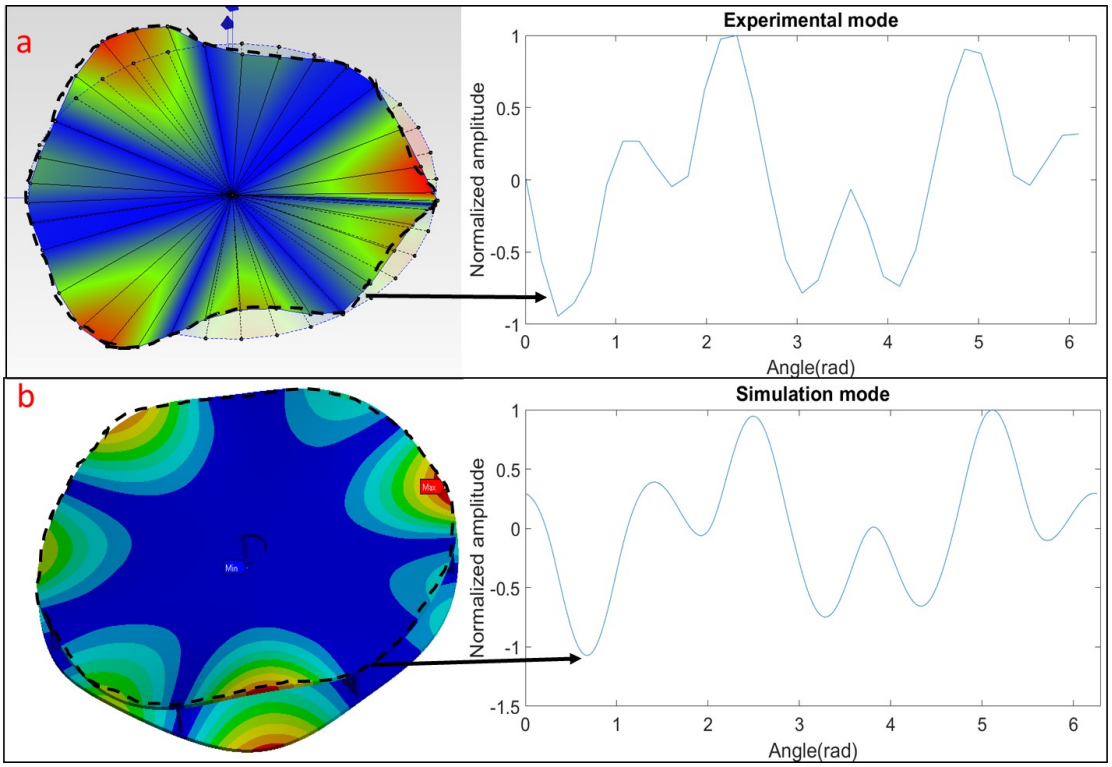


**Figure 12.** Response of the periphery for the same diametrical mode (326 Hz and second mode). (**a**) Experimental, (**b**) Numerical simulation.

Figure 12b shows the mode shape obtained with numerical simulation, which is based on a modal analysis of the bladed-disk using a FEM (Finite Element Method) Model with commercial software ANSYS [37]. A tetrahedral mesh, using SOLID186 [37] elements, was used for the calculation. A mesh sensitivity analysis was conducted, changing the number of elements of the mesh such that it does not affect the results. The optimal mesh had 20940 elements. The results obtained show good accuracy of the experimentation in natural frequency values. For the simulation, the response on the periphery is obtained in 225 points due to mesh discretization.

In order to compare both experimental and simulation results, the amplitude is normalized in both cases. The comparison between experimental and simulation results for the periphery of the analyzed modes (Figure 11) is shown in Figure 13. In the same figure, the decomposition of the mode shape, according to the method presented in Section 3, is also shown for both experimentation and simulation procedures.

It is seen that there is a good correlation between the experimental and numerical results. The peripheral deformation is quite similar for the analyzed modes, and the main diametrical components detected for each mode shape are the same, when analyzing the disk-blades-disk assembly experimentally and numerically. The MPC (Modal Phase Collinearity) [2] close to one (experimental results) shows that the mode shapes are real mode shapes (all points moving in phase or counterphase to each other). For the simulation, this is automatically achieved, since no damping effects are considered (undamped system) and, therefore, the modes are real. The discrepancy in natural frequencies values (between experimental and numerical results) is less than 7% for the analyzed modes.

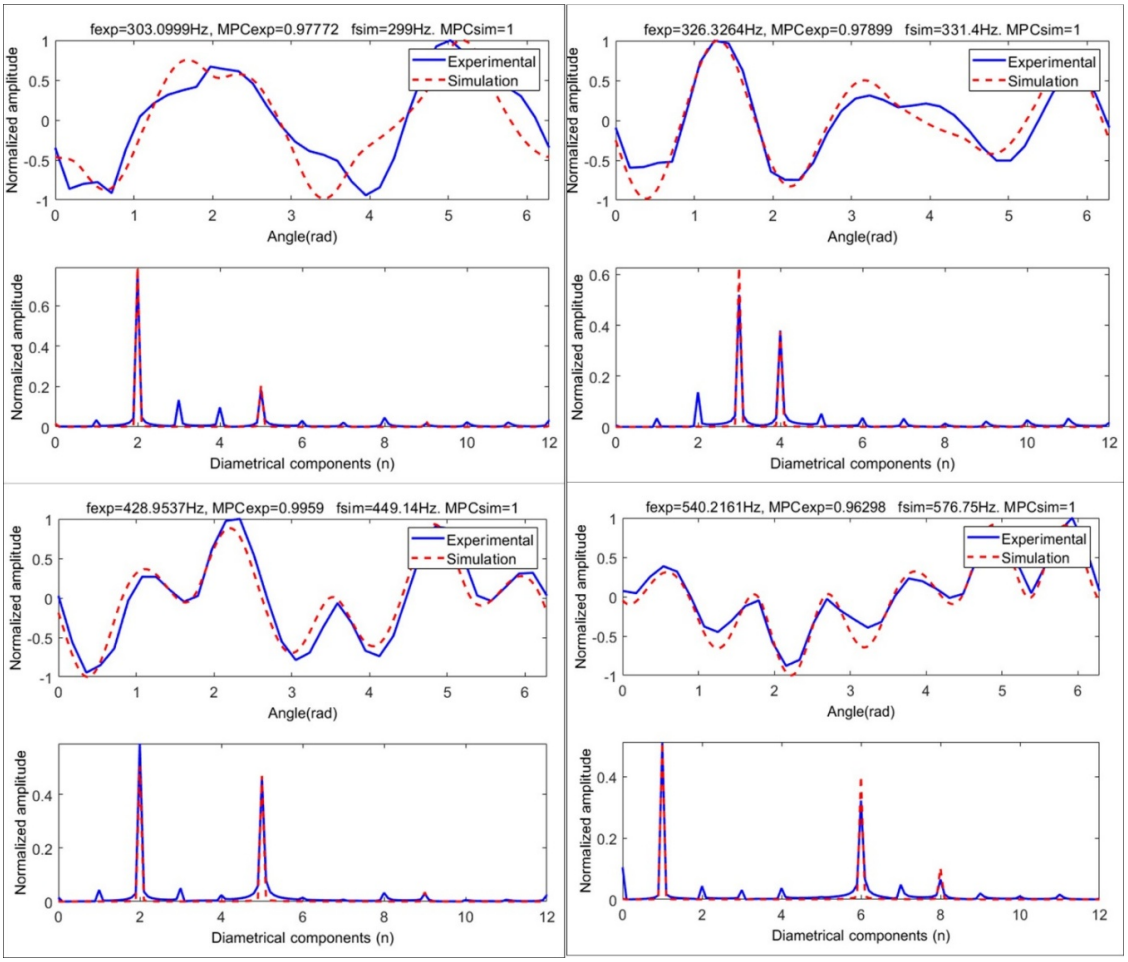


**Figure 13.** Diametrical modes analyzed with experimentation and simulation. Peripheral deformation and mode shape decomposition.

### *5.3. Tests with the Disk-Blades-Disk Structure Rotating and Detection of Natural Frequencies with LDV from the Stationary Frame*

To determine which peaks, corresponding to the first natural frequencies of the rotating structure (diametrical mode shapes), are obtained with a stationary sensor (LDV), the following procedure is used. The rotating speed of the structure is fixed as 5 Hz. In this condition, the disk-blades-disk structure is excited with a harmonic excitation (pure sine), created with the exciter PZT. Each of the analyzed diametrical modes in this paper (Figure 13) is excited. The response is simultaneously measured with the PZT attached to the rotating structure (sensor) and with the LDV on the stationary frame. Figure 14 shows the excitation and response from both rotating and stationary frames for the third mode analyzed (Figure 11).

From the time signals, it is observed that, when the excitation starts (Figure 14a), the dynamic response of the rotating structure is clearly affected, as seen on the rotating frame sensor. This response is clearly dominated by the excitation signal. From the stationary frame (LDV), a change in signal behavior is also appreciated during the time of the excitation. The response observed with the LDV during that time is the superposition of the response due to the PZT-excitation and the response due to the low frequency motion of the rotating structure. This motion, which is mainly due to imperfections on the surface and misalignment of the rotating structure, produces low frequency components around the rotating speed of the disk and first harmonics when the structure rotates [19,48]. Nevertheless, for the frequency range of the analyzed diametrical modes, only residual harmonics can be appreciated. These harmonics are not important in comparison with the level of peaks caused by the excitation of the natural frequencies (Figure 14b (LDV response)).

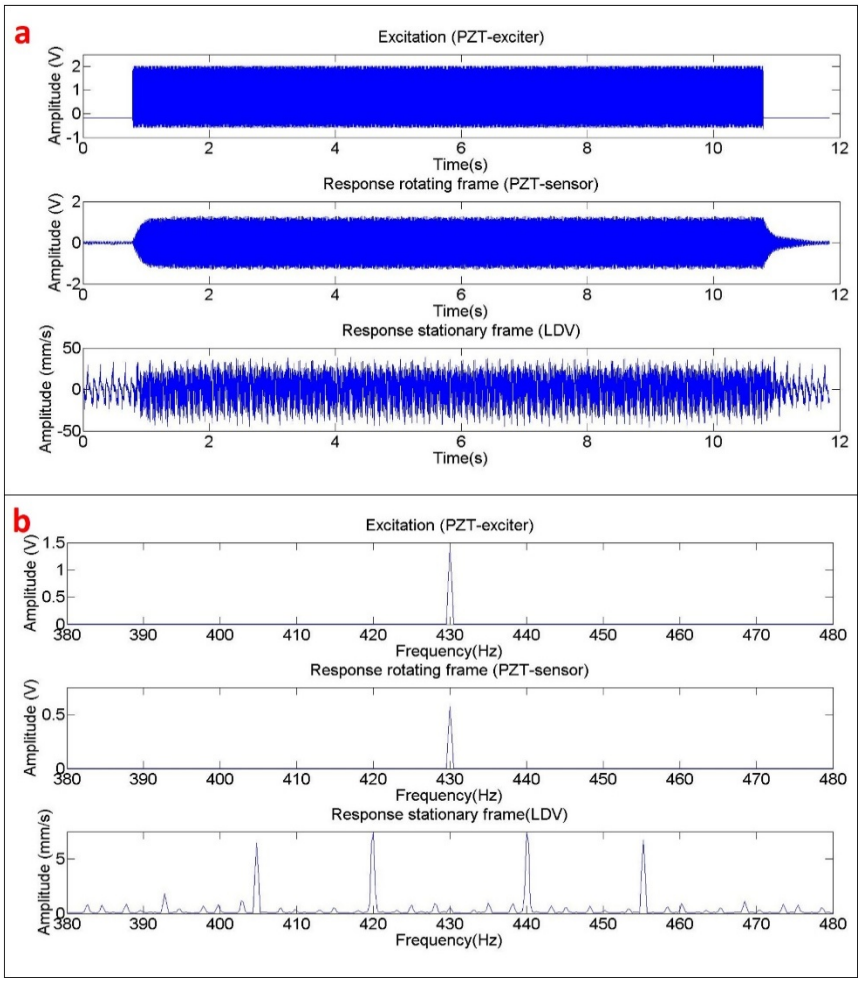


**Figure 14.** Excitation and response of the bladed-disk when exciting the third mode of Figure 11 PZT exciter, PZT sensor and LDV. (**a**) Time signals (**b**) Autospectrum.

Analyzing the response from the rotating frame in the frequency domain (Figure 14b (PZT)), it can be seen that only the excited frequency, which is a natural frequency of the structure, appears. Furthermore, from the stationary frame, the frequencies detected are symmetrically shifted with respect to the excited frequency.

It is to be mentioned that due to the rotation, the exact value of some natural frequencies experiences a slight increase [43,49], with respect to the stationary case. This increase is less than 2 Hz (0.5%) with respect to the non-rotating case value, for all the analyzed diametrical modes (Figure 11).

To relate the frequency modulations and the diametrical components detected with the mode shape decomposition, the following transformation in the frequency axis is performed for each of the *i*-analyzed diametrical modes:

$$f_{norm} = \frac{f - f_{excited}}{\Omega} \tag{15}$$

$f$ represents all the x-axis values (Figure 14), $f_{excited}$ is the frequency excited with the patch (the natural frequency from the rotating frame) and $\Omega$ the rotating speed of the disk-blades-disk structure (which is always 5 Hz in these paper). This transformation gives the frequency content of the response in terms of the diametrical components since it is precisely what it is obtained isolating $n$ from Equation (13).

To normalize the amplitude of the vibration of the rotating sensor (PZT) and of the stationary sensor (LDV), the following procedure is used. For the bladed-disk with no rotation, the same harmonic excitation as in the rotating case (in some cases reducing 1 or 2 Hz the excited frequency due to

the slight increase in the natural frequency values [43,49], when the structure rotates) is applied to the disk-blades-disk structure. The LDV, in this case, focuses on the point with maximal peripheral deformation, which is determined by the modal analysis performed in the previous section. This test gives the values $A_{PZT,\ \Omega=\ 0\text{Hz},f=fexcited}$ and $A_{LDV,\ \Omega=\ 0\text{Hz},f=fexcited}$ for each of the analyzed modes, which are the amplitude of the response of the bladed-disk at the natural frequency considered ($f_{excited}$). Therefore, for each of these $i$-modes:

$$A_{norm,PZT} = \frac{A_{PZT,\Omega=\ 5\text{Hz}}}{A_{PZT,\Omega=\ 0\text{Hz},f=fexcited}}, A_{norm,LDV} = \frac{A_{LDV,\Omega=\ 5\text{Hz}}}{A_{LDV,\Omega=\ 0\text{Hz},f=fexcited}} \tag{16}$$

Note that $A_{PZT,\ \Omega=\ 5\text{Hz}}, A_{LDV,\ \Omega=\ 5\text{Hz}}$ represent all the values of the spectra shown in Figure 14 and $A_{PZT,\ \Omega=\ 0\text{Hz},f=fexcited}$, $A_{LDV,\ \Omega=\ 0\text{Hz},f=fexcited}$ are just single numbers. The normalization of the amplitude compares the amplitudes obtained with the PZT (Rotating Frame) and the LDV (Stationary Frame), and sees if they are in accordance with Equation (14). As an example, the normalization in frequency and amplitude of the mode analyzed in Figure 14 is shown in Figure 15.

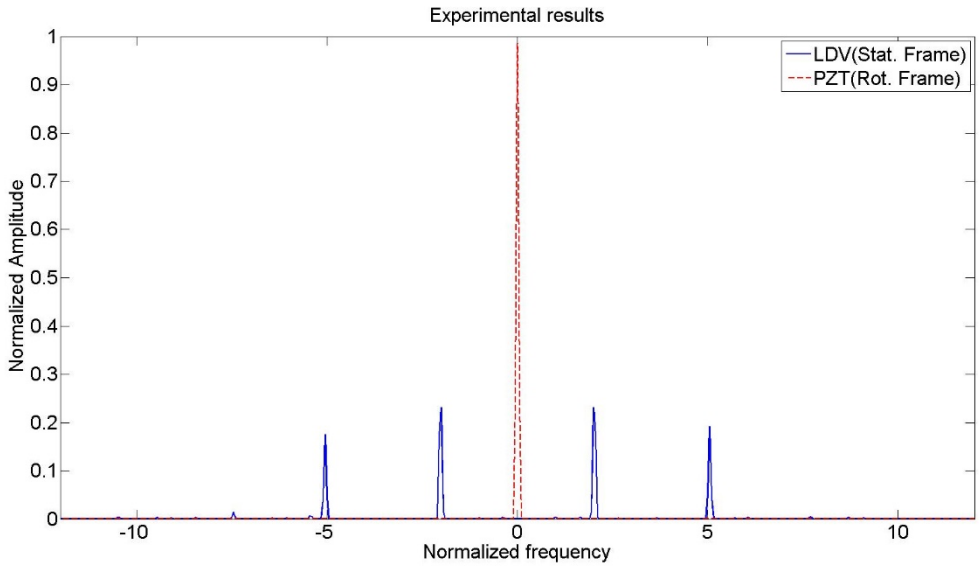


**Figure 15.** Normalized response of the PZT and LDV for the third mode in Figure 11.

As deduced in Section 4, the experimental frequencies obtained from the stationary frame are directly related to the mode shape decomposition method proposed in this paper. Therefore, the decomposition in diametrical components of the peripheral deformation obtained with experimental and numerical modal analysis (Section 5.2) is necessary to understand what is obtained from the stationary frame. For this purpose, the mode shape decompositions of the analyzed modes (Figure 13) are simply separated into a negative and positive part, according to Equation (14).

Therefore, if A(n) is considered as the function obtained with the mode shape decomposition (functions shown in Figure 13), the following function $A'(n)$ can be calculated, for each of the analyzed $i$-modes, according to:

$$A'(n) = \frac{A(|n|)}{2} \tag{17}$$

$A'(n)$, which is defined for positive and negative $n$, can be directly compared with the experimental results obtained with the LDV, for the rotating disk-blades-disk, after having normalized the Frequency and Amplitude (Equations (15) and (16)). This is performed for all the diametrical modes analyzed in this paper obtaining Figure 16.

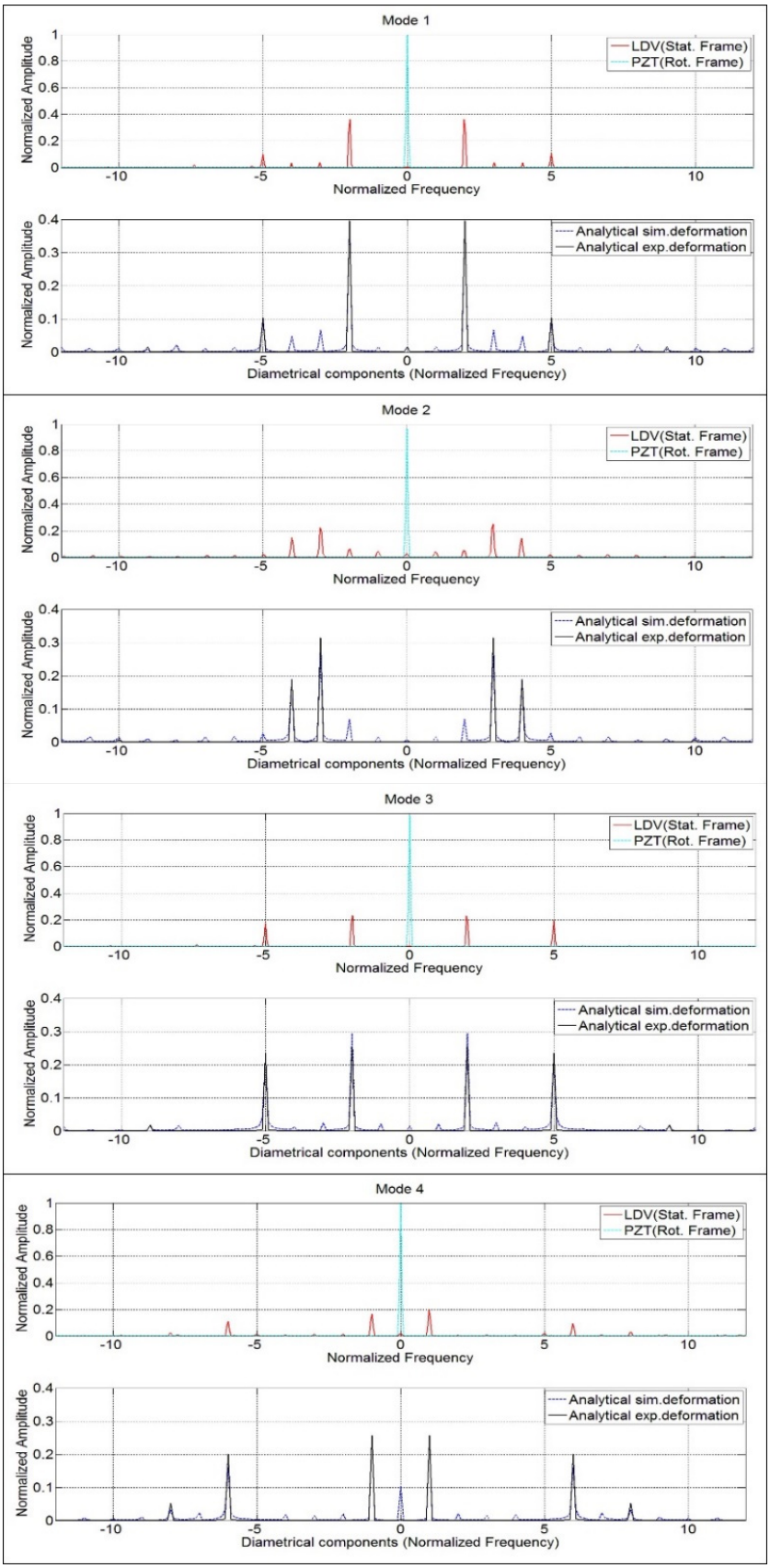


**Figure 16.** Experimental results for the frequencies detected with the stationary sensor (LDV) and its relationship to the diametrical components obtained with the mode shape decomposition.

As seen in Figure 16, the main components obtained with the mode shape decomposition are closely related to the natural frequencies of the rotating structure that are observed from the stationary frame. This means that the frequencies observed from the stationary frame can be predicted with the method proposed for the mode shape decomposition.

Furthermore, the amplitudes for the experimental results are slightly lower than the ones predicted with the mode shape decomposition. These differences can be attributed to the experimental fact that rough surfaces and misalignment can cause a loss of the returned light to the Laser lens. These effects, known as speckle noise and pseudo-vibrations, have been discussed in many references [50–53]. To quantify these effects, the predominant component of each of the analyzed modes is considered, and the amplitudes experimentally detected with the Laser and those ones analytically predicted are compared. In this case, the average amplitude detected with the Laser is around 20% less than the amplitude analytically predicted.

Therefore, in this section, the utility of the mode shape decomposition has been demonstrated to predict the natural frequencies observed by a sensor on the stationary frame, when the rotating disk-blades-disk structure is under resonance condition of a diametrical mode.

### *5.4. Limitation of Standard Numerical Codes For Non-Axisymmetric Rotating Structures Analyzed in the Stationary Frame*

It is important to mention that such behavior is not well predicted when using commercial software that restrict rotating structures to be axisymmetric around the rotating axis (ANSYS®, Canonsburg, PA [37], MSC NASTRAN®, Newport Beach, CA [38]). For this reason, frequencies from the stationary frame of simple axisymmetric disk structures have been successfully predicted in the past [54], while for non- axisymmetric structures, such as the structure analyzed here, this is not possible if the same kind of numerical simulations are performed.

This is shown in Figure 17, where the prediction of peaks and relative amplitudes detected with a stationary sensor, when a resonance of the first diametrical mode of the rotating structure occurs, is compared for different methods. Two cases are considered here: the first diametrical mode shape of a simple disk with $n = 2$ (and no nodal diameters) [19] and the first diametrical mode shape of the present disk-blades-disk structures (with main component $n = 2$). The different methods are compared with experimental results. Simple disk theory means that in Equation (14), only the main diametrical component $n$ is considered and therefore only two peaks, with half amplitude and modulated $n{\cdot}\Omega$, are predicted. Direct simulation means to introduce a rotating speed to the disk or disk-blades-disk structure and obtain the frequencies from the stationary frame (using ANSYS standard code [37]). The mode shape decomposition is applied to discompose the mode shape obtained in the standing case by means of experimental modal analysis and numerical modal analysis, as explained in this paper.

As seen in this figure, for the simple disk, all the predictions accurately determine the amplitude and frequency of the peaks of the stationary sensor and, therefore, the proposed method in this paper does not offer extra relevant information for simple disk structures. Nevertheless, for the disk-blade-disk assembly, the simple disk theory predicts only two peaks with higher amplitude, as the description of the mode shape is incomplete. Direct simulation with a standard code also fails, as axisymmetric structures are required. In this case, only the mode-shape decomposition, proposed in this paper, approaches the experimental results obtained.

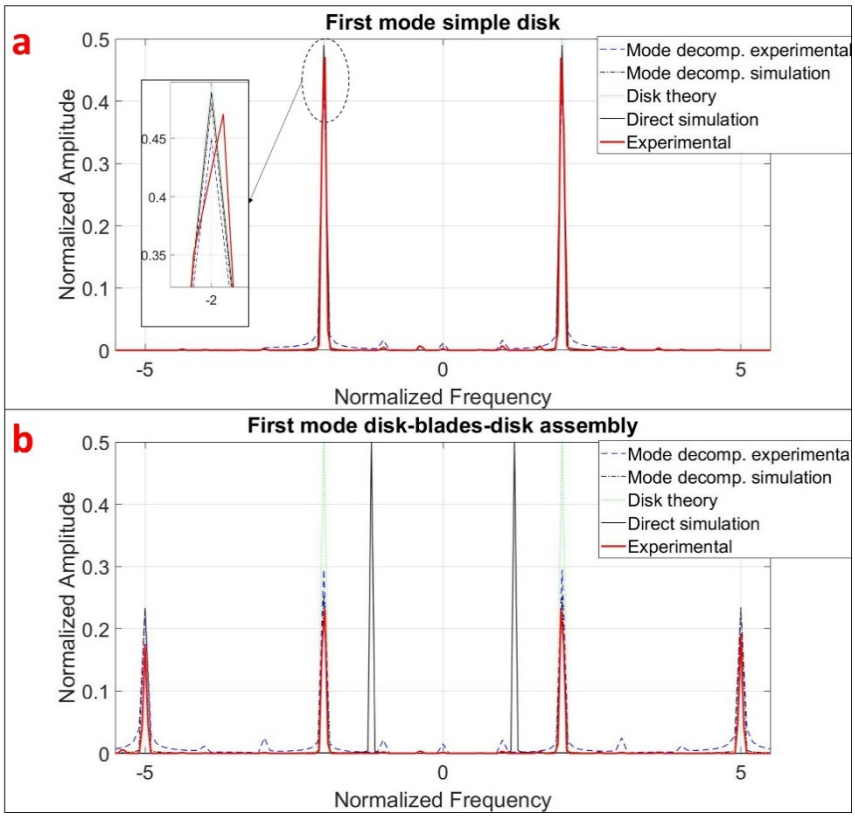


**Figure 17.** Peak prediction (direct simulation (ANSYS), mode shape decomposition method (experimental and numerical mode shape), simple disk theory) and experimental results for the stationary frame and mode shape with main component $n = 2$: (**a**) simple disk structure [19], and (**b**) disk-blades-disk assembly.

### *5.5. Validity of the Relationship between the Mode Shape Decomposition and the Frequencies Detected from the Stationary Frame and Future Work*

In this section, we have shown that the proposed method allows to predict the frequencies and relative amplitudes of the different peaks seen by a stationary sensor, for the typical range of rotating speeds of prototypes consisting of a disk-blade-disk assembly. The effects of the relative rotation of a surrounding heavy fluid, such as water (the normal fluid in the operation of hydropower units), which have been discussed in previous papers [19,43,55], are not considered in this case and will be analyzed in a future paper. The validity of this analysis is therefore for large centrifugal compressors (which work in air and with relative low rotating speed) and hydropower units working in synchronous condenser mode [56,57], and serve as a basis for future considerations of the effect of a surrounding heavy fluid (water) in hydropower units.

## 6. Conclusions

In this paper, an analysis of the natural frequencies and mode shapes of disk-blade-disk assemblies from a stationary frame and in relation to the mode shapes that characterize simple disks has been discussed. The experimental results and methodology followed has relevant interest due to the use of these assemblies (disk-blades-disk) in real impellers (closed impellers) of centrifugal compressors, centrifugal pumps, pump-turbines, and low specific speed Francis runners.

A method to discompose and characterize the several first mode shapes of disk-blade-disk assemblies (vibration modes with a maximum deformation in the periphery and no nodal diameters) is proposed. The peripheral deformation of these mode shapes, which can be obtained by means of

experimental or numerical modal analysis of the standing structure, is expressed as the superposition of diametrical mode shapes that characterize simple disks after the used decomposition.

For such structures rotating in the typical range of turbomachinery prototypes, it has been shown that such decomposition allows to predict the frequencies and amplitudes of the corresponding peaks detected with a stationary sensor. As discussed and shown in this paper, this is not possible with standard numerical codes, which typically have a restriction of axisymmetric structures for analyses in the stationary frame.

Finally, the decomposition method and analysis in this paper serves as a basis for a future work, where the effect of a heavy surrounding fluid with relative rotation on the structure (normal operating conditions in hydropower units) will be discussed.

**Author Contributions:** A.P., D.V., C.V. and E.E. conceived and designed the experiments; A.P. performed the experiments; M.E. and E.E. revised the manuscript; A.P. wrote the paper.

**Funding:** This research received no external funding.

**Acknowledgments:** The authors wish to acknowledge Voith Hydro Holding GmbH & Co. KG for the technical and economic support. Alexandre Presas acknowledges the Serra Hunter program of Generalitat de Catalunya.

**Conflicts of Interest:** The authors declare no conflict of interest.

## References

1. Ewins, D.J. *Modal Testing: Theory and Practice*; Research Studies Press Letchworth: Letchworth Garden City, UK, 1984; Volume 15.
2. Heylen, W. *Modal Analysis Theory and Testing*; Katholieke Universiteit Leuven: Leuven, Belgium, 2007.
3. Bucher, I. Transforming and separating rotating disk vibrations using a sensor array. *J. Sound Vib.* **2011**, *330*, 1244–1264. [CrossRef]
4. Legrand, M.; Pierre, C.; Cartraud, P.; Lombard, J.-P. Two-dimensional modeling of an aircraft engine structural bladed disk-casing modal interaction. *J. Sound Vib.* **2009**, *319*, 366–391. [CrossRef]
5. Singh, M.P.; Thakur, B.K.; Sullivan, W.E.; Donald, G. Resonance identification for impellers. In Proceedings of the 32nd Turbomachinery Symposium, College Station, TX, USA, 8–11 September 2003; A&M University. Turbomachinery Laboratories: College Station, TX, USA, 2003.
6. Egusquiza, E.; Valero, C.; Presas, A.; Huang, X.; Guardo, A.; Seidel, U. Analysis of the dynamic response of pump-turbine impellers. Influence of the rotor. *Mech. Syst. Signal Process.* **2016**, *68–69*, 330–341. [CrossRef]
7. Southwell, R.V. On the free transverse vibrations of a uniform circular disc clamped at its centre and on the effects of rotation. *Proc. R. Soc. Lond.* **1922**, *101*, 133–153. [CrossRef]
8. Belvins, R. *Formulas for Natural Frequency and Mode Shape*; Krieger Publishing Company: Malabar, FL, USA, 1984.
9. Leissa, A.W. *Vibration of Plates*; Goverment Printing Office: Washington, DC, USA, 1969.
10. Vogel, S.; Skinner, D. Natural frequencies of transversely vibrating uniform annular plates. *J. Appl. Mech.* **1965**, *32*, 926–931. [CrossRef]
11. Rao, S.S.; Prasad, A. Vibrations of annular plates including the effects of rotatory inertia and transverse shear deformation. *J. Sound Vib.* **1975**, *42*, 305–324. [CrossRef]
12. Weisensel, G. Natural frequency information for circular and annular plates. *J. Sound Vib.* **1989**, *133*, 129–137. [CrossRef]
13. Leissa, A.; Narita, Y. Natural frequencies of simply supported circular plates. *J. Sound Vib.* **1980**, *70*, 221–229. [CrossRef]
14. Amabili, M.; Forsali, G.; Kwak, M.K. Free vibrations of annular plates coupled with fluids. *J. Sound Vib.* **1996**, *191*, 825–846. [CrossRef]
15. Amabili, M. Effect of finite fluid depth on the hydroelastic vibration of circular and annular plate. *J. Sound Vib.* **1996**, *193*, 909–925. [CrossRef]
16. Mehdigholi, H. Forced Vibration of Rotating Discs and Interaction with Non-Rotating Structures. Ph.D. Thesis, Imperial College, London, UK, 1991.
17. Ahn, T.K.; Mote, C.D. Mode Identification of a Rotating Disk. *Exp. Mech.* **1998**, *38*, 250–254. [CrossRef]

18. Chung, J.; Kang, N.-C.; Lee, J.M. A study on free vibration of a spinning disk. *KSME J.* **1996**, *10*, 138–145. [CrossRef]
19. Presas, A.; Valentin, D.; Egusquiza, E.; Valero, C.; Seidel, U. On the detection of natural frequencies and mode shapes of submerged rotating disk-like structures from the casing. *Mech. Syst. Signal Process.* **2015**, *60*, 547–570. [CrossRef]
20. Ewins, D. Vibration characteristics of bladed disc assemblies. *J. Mech. Eng. Sci.* **1973**, *15*, 165–186. [CrossRef]
21. Castanier, M.P.; Pierre, C. Modeling and analysis of mistuned bladed disk vibration: Current status and emerging directions. *J. Propuls. Power* **2006**, *22*, 384–396. [CrossRef]
22. Ottarsson, G.; Castanier, M.; Pierre, C. A reduced-order modeling technique for mistuned bladed disks. In Proceedings of the 35th Structures, Structural Dynamics, and Materials Conference, Hilton Head, SC, USA, 18–20 April 1994; p. 1640.
23. Jacquet-Richardet, G.; Ferraris, G.; Rieutord, P. Frequencies and modes of rotating flexible bladed disc-shaft assemblies: A global cyclic symmetry approach. *J. Sound Vib.* **1996**, *191*, 901–915. [CrossRef]
24. Lemeš, S.; Zaimović-Uzunović, N. Mode shapes of centrifugal pump impeller. In Proceedings of the 6th International Research/Expert Conference on Trends in the Development of Machinery and Associated Technology (TMT 2002), Neum, Bosnia and Herzegovina, 18–22 September 2002.
25. Wang, Q.; Bartos, J.C.; Houston, R.A. Methodology of open bladed impeller resonance indentification. In Proceedings of the 28th Turbomachinery Symposium, College Station, TX, USA, September 1999; A&M University. Turbomachinery Laboratories: College Station, TX, USA, 1999.
26. Lais, S.; Liang, Q.; Henggeler, U.; Weiss, T.; Escaler, X.; Egusquiza, E. Dynamic Analysis of Francis Runners—Experiment and Numerical Simulation. *Int. J. Fluid Mach. Syst.* **2009**, *2*, 303–314. [CrossRef]
27. Tanaka, H. Vibration Behavior and Dynamic Stress of Runners of Very High Head Reversible Pump-turbines. *Int. J. Fluid Mach. Syst.* **2011**, *4*, 289–306. [CrossRef]
28. Kubota, Y.; Susuki, T.; Tomita, H.; Nagafuji, T.; Okamura, T. Vibration of rotating bladed disc excited by stationary distributed forces. *Bull. JSME* **1985**, *26*, 1952–1957. [CrossRef]
29. Kubota, Y.; Ohashi, H. A study on the natural frequencies of hydraulic pumps. In Proceedings of the 1st ASME Joint International Conference on Nuclear Engineering, Tokyo, Japan, 4–7 November 1991; pp. 589–593.
30. Egusquiza, E.; Valero, C.; Huang, X.; Jou, E.; Guardo, A.; Rodriguez, C. Failure investigation of a large pump-turbine runner. *Eng. Fail. Anal.* **2012**, *23*, 27–34. [CrossRef]
31. Escaler, X.; Hütter, J.K.; Egusquiza, E.; Farhat, M.; Avellan, F. Modal behavior of a reduced scale pump-turbine impeller. Part 1: Experiments. In Proceedings of the IOP Conference Series: Earth and Environmental Science, Timişoara, Romania, 20–24 September 2010; Iop Publishing: Bristol, UK, 2012; Volume 12, p. 012116.
32. Valero, C.; Huang, X.; Egusquiza, E.; Farhat, M.; Avellan, F. Modal behavior of a reduced scale pump turbine impeller. Part II: Numerical simulation. In Proceedings of the IOP Conference Series: Earth and Environmental Science, Timişoara, Romania, 20–24 September 2010; Iop Publishing: Bristol, UK, 2012; Volume 12, p. 012117.
33. Huang, X.X.; Egusquiza, E.; Valero, C.; Presas, A. Dynamic behaviour of pump-turbine runner: From disk to prototype runner. In Proceedings of the IOP Conference Series: Materials Science and Engineering, Beijing, China, 19–22 September 2013; IOP Publishing: Bristol, UK, 2013; Volume 52, p. 022036.
34. De Siervo, F.; De Leva, F. Modern trends in selecting and designing Francis turbines. *Water Power Dam Constr.* **1976**, *28*, 28–35.
35. Zobeiri, A. Investigations of Time Dependent Flow Phenomena in a Turbine and a Pump-Turbine of Francis Type: Rotor Stator Interactions and Precessing Vortex Rope. Ph.D. Thesis, École polytechnique fédérale de Lausanne (EPFL), Lausanne, France, 2009.
36. Nicolet, C.; Ruchonnet, N.; Avellan, F. One-dimensional modeling of rotor stator interaction in Francis Pump-Turbine. In Proceedings of the 23rd IAHR Symposium, Yokohama, Japan, 17–21 October 2006.
37. Inc, A. *ANSYS Mechanical APDL Theory Reference*; ANSYS, Inc.: Canonsburg, PA, USA, 2016; Volume 17.
38. Software, M. *MSC Nastran 2016. Rotordynamics User's Guide*; MSC: Newport Beach, CA, USA, 2016.
39. Chandraker, A. Runner Blade for Low Specific Speed Francis Turbine. US7210904B2, 1 May 2007.
40. Presas, A.; Valero, C.; Huang, X.; Egusquiza, E.; Farhat, M.; Avellan, F. Analysis of the Dynamic Response of Pump-Turbine Runners-Part I: Experiment. In Proceedings of the IOP Conference Series: Earth and Environmental Science, Beijing, China, 13–23 August 2012; IOP Publishing: Bristol, UK, 2012; p. 052015.

41. Anagnostopoulos, J.S. CFD analysis and design effects in a radial pump impeller. *WSEAS Trans. Fluid Mech.* **2006**, *1*, 763.
42. Richards, S.K.; Ramakrishnan, K.; Shieh, C.M.; Moyroud, F.; Picavet, A.; Ballarini, V.; Michelassi, V. Unsteady acoustic forcing on an impeller due to coupled blade row interactions. *J. Turbomach.* **2012**, *134*, 061014. [CrossRef]
43. Presas, A.; Valentin, D.; Egusquiza, E.; Valero, C.; Seidel, U. Influence of the rotation on the natural frequencies of a submerged-confined disk in water. *J. Sound Vib.* **2015**, *337*, 161–180. [CrossRef]
44. Lamb, H.; Southwell, R.V. The vibrations of spinning discs. *Proc. R. Soc. Lond.* **1921**, *99*, 272–280. [CrossRef]
45. Oppenheim, A.V. *Discrete-Time Signal Processing*; Pearson Education India: Chennai, India 1999.
46. Heath, S.; Imregun, M. A Review of Analysis techniques for blade tip-timing measurements. In Proceedings of the ASME 1997 International Gas Turbine and Aeroengine Congress and Exhibition, Orlando, FL, USA, 2–5 June 1997.
47. Bi, S.; Ren, J.; Wang, W.; Zong, G. Elimination of transducer mass loading effects in shaker modal testing. *Mech. Syst. Signal Process.* **2013**, *38*, 265–275. [CrossRef]
48. Egusquiza, E.; Valero, C.; Valentin, D.; Presas, A.; Rodriguez, C.G. Condition monitoring of pump-turbines. New challenges. *Measurement* **2015**, *67* (Suppl. C), 151–163. [CrossRef]
49. Bauer, H.F.; Eidel, W. Transverse vibration and stability of spinning circular plates of constant thickness and different boundary conditions. *J. Sound Vib.* **2007**, *274*, 877–895. [CrossRef]
50. Vass, J.; Šmíd, R.; Randall, R.; Sovka, P.; Cristalli, C.; Torcianti, B. Avoidance of speckle noise in laser vibrometry by the use of kurtosis ratio: Application to mechanical fault diagnostics. *Mech. Syst. Signal Process.* **2008**, *22*, 647–671. [CrossRef]
51. Martin, P.; Rothberg, S.J. Pseudo-vibration sensitivities for commercial laser vibrometers. *Mech. Syst. Signal Process.* **2011**, *25*, 2753–2765. [CrossRef]
52. Rothberg, S. Numerical simulation of speckle noise in laser vibrometry. *Appl. Opt.* **2006**, *45*, 4523–4533. [CrossRef] [PubMed]
53. Rothberg, S.J.; Halkon, B.J.; Tirabassi, M.; Pusey, C. Radial vibration measurements directly from rotors using laser vibrometry: The effects of surface roughness, instrument misalignments and pseudo-vibration. *Mech. Syst. Signal Process.* **2012**, *33*, 109–131. [CrossRef]
54. Valentín, D.; Presas, A.; Egusquiza, E.; Valero, C. On the Capability of Structural–Acoustical Fluid–Structure Interaction Simulations to Predict Natural Frequencies of Rotating Disklike Structures Submerged in a Heavy Fluid. *J. Vib. Acoust.* **2016**, *138*, 034502. [CrossRef]
55. Presas, A.; Valentin, D.; Egusquiza, E.; Valero, C.; Seidel, U. Dynamic response of a rotating disk submerged and confined. Influence of the axial gap. *J. Fluids Struct.* **2016**, *62*, 332–349. [CrossRef]
56. Vagnoni, E.; Andolfatto, L.; Avellan, F. On the sloshing free surface in the draft tube cone of a Francis turbine operating in synchronous condenser mode. *J. Phys. Conf. Ser.* **2017**, *813*, 012034. [CrossRef]
57. Vagnoni, E.; Favrel, A.; Andolfatto, L.; Avellan, F. Experimental investigation of the sloshing motion of the water free surface in the draft tube of a Francis turbine operating in synchronous condenser mode. *Exp. Fluids* **2018**, *59*, 95. [CrossRef]